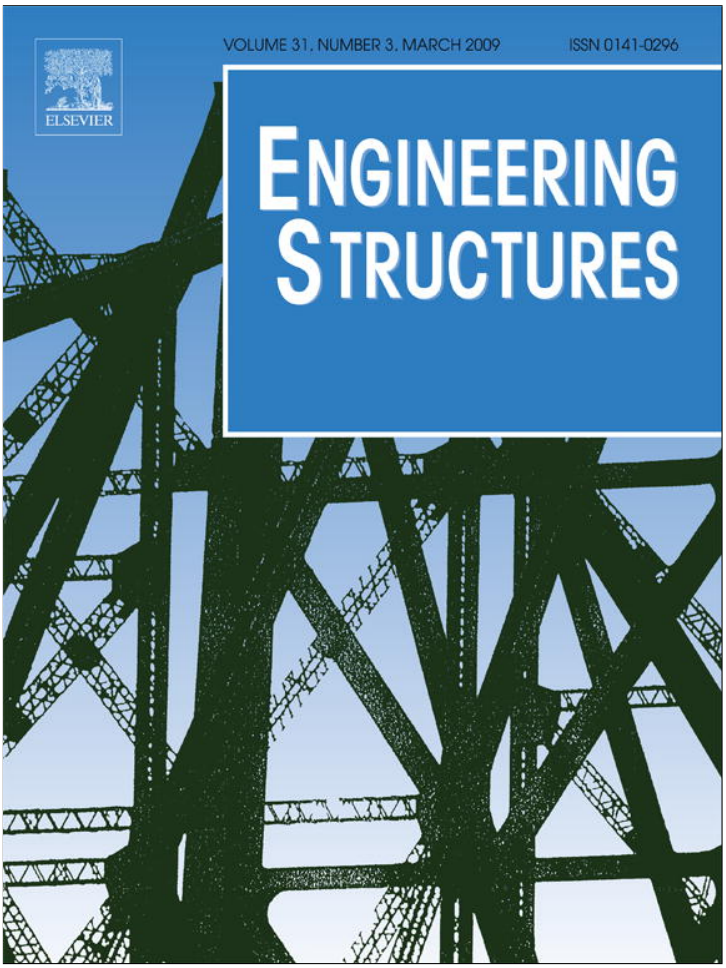

Engineering Structures 31 (2009) 729–737

Contents lists available at ScienceDirect

Engineering Structures

journal homepage: www.elsevier.com/locate/engstruct

Soil–structure interaction effects on base-isolated buildings founded on soil stratum

C.C. Spyrakos *, Ch.A. Maniatakis, I.A. Koutromanos

Department of Civil Engineering, Laboratory for Earthquake Engineering, National Technical University of Athens, GR-15700 Zografos, Athens, Greece

ARTICLE INFO

Article history:
Received 24 June 2008
Received in revised form
8 August 2008
Accepted 3 October 2008
Available online 1 January 2009

Keywords:
Multistory building
Seismic response
Soil–structure interaction
Base isolation

ABSTRACT

The present study investigates the effects of soil–structure interaction (SSI) on the response of base-isolated multistory buildings founded on an elastic soil layer overlying rigid bedrock and subjected to a harmonic ground motion. Initially a four-degree-of-freedom system (4-DOF) is developed and the equations of motion are formulated in the frequency domain. Frequency independent expressions are used to determine the stiffness and damping coefficients for the rigid surface foundation on the soil-stratum underlined by bedrock at shallow depth. Assuming the foundation mass to be negligible, an equivalent two-degree-of-freedom (2-DOF) system is derived. The first mode of motion of the equivalent 2-DOF system appears to be sufficient to describe the response of the overall system for all ranges of stiffness and inertia properties of the structure and its isolation. An extensive parametric study demonstrates that SSI effects are significant, primarily for squat, light structures, founded on soil-stratum of low stiffness. The methodology could serve as a means to perform a preliminary seismic design of base-isolated building structures founded on homogenous soil-stratum over bedrock.

1. Introduction

Base isolation intends to uncouple the structure from seismic ground motion, minimizing, simultaneously, the interstory deformations and the floor accelerations by interposing elements of high axial and low horizontal stiffness between the structure and the foundation. Even though the concept of base isolation has been introduced from the beginning of the 19th century, it has been extensively studied and applied to engineering practice only during the last 25 years. From the application of a rubber isolation system by Swiss engineers in 1969 [1] to the 1991 Uniform Building Code [2] that included provisions for base-isolated buildings and the seismic retrofitting of the San Francisco City Hall in the late nineties [3], many researchers have contributed to the attained level of knowledge, e.g. [4–7].

In recent years, the impact of long-period pulses on the displacement demands of isolators for structures built at near-fault sites has been studied. In a recent study, Jangid and Kelly [8] have compared the response of isolation systems in near-source regions, while other researchers have suggested use of additional energy dissipative mechanisms [9–12]. Ryan and Chopra [13] have studied the eccentricity effect on the response of base-isolated buildings with an asymmetrical plan; later, they investigated the peak lateral bearing deformation of base-isolated structures with a procedure that takes into account the overturning effect [14]. Today, thorough specifications for the seismic design of isolated structures are included in several scientific textbooks [15] and Code Provisions [16,17].

Consideration of fixed-base support is proved to be valid only for structures founded on rock or soil of high stiffness. In general, the interaction between soil and structure results in a decrease of the fundamental frequency of the response and a modification in the energy dissipation, which is attributed to radiation and material damping in the soil [18]. Soil–structure interaction has captured the interest of many researchers from the late '70s, e.g., [19–21] who contributed to the clarification of a large number of issues concerning the application of SSI to engineered structures, especially nuclear power plants. Both analytical [22,23] and numerical [24] procedures have been used to study pertinent parameters that affect SSI on a variety of structures, e.g., [25–29]. Seismic Code Provisions, such as the FEMA 450 [30] suggest consideration of SSI for the seismic design of structures. Also, simple criteria have been established to account for SSI in engineering practice, e.g., [31].

The coupled effect of SSI and base isolation on structures has gained the interest of researchers during the last few years. Soil–structure interaction has been mainly considered for base-isolated bridges and liquid storage tanks. In a parametric study, Spyrakos and Vlassis [32] have assessed the effects of SSI on the response of base-isolated bridges. Analytical expressions have been derived to demonstrate the significance of SSI phenomena

* Corresponding author. Tel.: +30 210 772 1187; fax: +30 210 772 1182.
E-mail address: spyrakos@hol.gr (C.C. Spyrakos).

0141-0296/$ – see front matter © 2008 Elsevier Ltd. All rights reserved.
doi:10.1016/j.engstruct.2008.10.012

in influencing the response of an isolated system, and the need to incorporate SSI in bridge design has been addressed.

Chaudhary et al. [33] have used simple lumped mass models to study the response of four base-isolated bridges and identify SSI effects. They compare recorded earthquake response data of bridge pier-caps and girders, with the corresponding free-field motion. The ratio of pier stiffness and horizontal foundation stiffness has been found to influence the extent of SSI effects rather than the soil shear modulus. The effectiveness of base isolation for bridge retrofitting has been studied by Iemura and Pradono [34] providing an insight to the role of damping. Frequency independent expressions have been used to model the foundation flexibility with the assumption of an elastic halfspace for the subsoil. Tongaonkar and Jangid [35] have studied the seismic response of both non-isolated and isolated bridges with elastomeric bearings, to show that ignoring SSI could lead to unconservative estimations of displacements at the abutments. They reported that the coupling effect of SSI and isolation in bridges significantly affects the total response of the bridge when the isolation bearings are nearly ten times stiffer than the supporting soil medium, while an increase in flexibility of bridge and bearings diminish the influence of SSI. The need to consider SSI in isolated bridges with a light superstructure and a heavy substructure, regardless the soil stiffness, has been ascertained by Dicleri et al. [36] assuming nonlinear behavior for the isolators. Sarrazin et al. [37] has provided extended results concerning the response of two base-isolated bridges in Chile. The beneficial effect of base isolation in reducing the longitudinal response amplitude is addressed. The assumption of rigid base appeared to be valid; however, further research is suggested, to clarify the significant difference between the response recorded at the bridge pier and the motion recorded at the free-field.

The destruction of liquid storage tanks during severe earthquakes in the United States and Japan and the increase in application of seismic-isolation techniques for their construction led to the investigation of the soil–structure–liquid interaction effects on the response of structures of this type [38,39]. Shenton and Hampton [40] have compared the response of fixed-base and isolated water tanks to demonstrate the effectiveness of base isolation in reducing the deformations, base shear and overturning moment, especially for tanks with low water capacity. Two studies by Kim et al. [41] and Cho et al. [42] provide information concerning the seismic response of isolated liquid storage tanks. According to these studies, the deformation and force-undertaking demands are reduced in tanks founded on soil of low stiffness. Also, important parameters affecting the response have been found to consist of the liquid filling ratio and the base isolator type.

The significant role of SSI on the response of base-isolated building structures is rather limited. An experimental study carried out at the University of California at Berkeley concerning base-isolated nuclear facilities founded on soft-soil sites has led to the conclusion that the isolator design should account for significant displacement demands [43]. Constantinou and Kneifati [44] have proposed a rather complex procedure and a less sophisticated energy method to estimate the damping of a seismically isolated structure, taking into account the energy dissipation of the bearings and the radiation damping in the soil. Novak and Henderson [45] have investigated the modal properties of base-isolated structures and have concluded that, when the flexibility of soil and isolators are comparable, the contribution of SSI should not be ignored. Tsai et al. [46] have developed a time-domain procedure to investigate the efficiency of isolators to reduce the energy imparted in an FPS-isolated building for earthquake motion. Both radiation damping and foundation flexibility are found to be essential in the accuracy of response prediction and safety of the isolated structure.

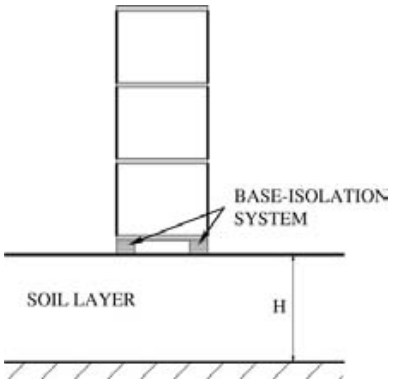

Fig. 1. Base-isolated structure founded on a shallow soil layer.

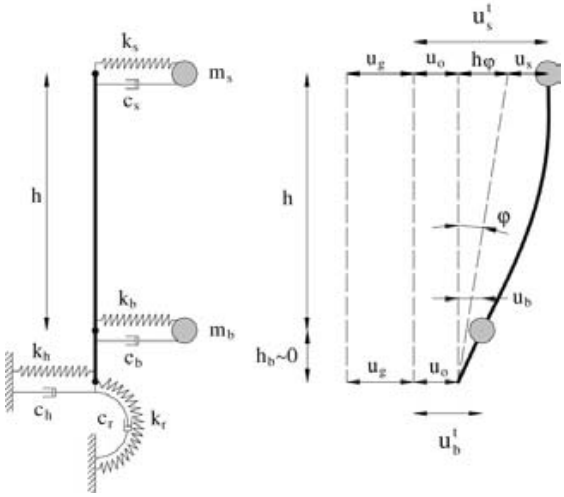

Fig. 2. Analytical model for base-isolated structure including soil impedances.

The objective of this paper is to extend the existing knowledge in the field of seismically isolated building structures, taking into account the role of SSI. The coupled effect of base isolation and SSI is studied with the aid of a simple analytical model. A parametric study is performed for an extensive range of structure, base isolator and soil characteristics. The methodology could be applied for preliminary analysis and design of base-isolated building structures accounting for the effects of SSI.

2. Equations of motion for the initial system

The study investigates the response of a multistory base-isolated building founded on an elastic soil layer with thickness H that overlies a stiff rock formation, as shown in Fig. 1. The building is either one-story or multistory with a distribution of stiffness and mass with height that allows a rather reliable study by means of an equivalent single-degree-of-freedom (SDOF) system [47]. The characteristics of the system can be determined by either the building first mode or a deformation pattern based on an anticipated response under seismic load, such as the inversed triangle displacement distribution with height.

The structure is assumed to remain elastic during base excitation. Under the assumption that the foundation system is massless, the equations of motion can be established with reference to Fig. 2. The structural, base isolation, translational and rotational foundation degrees-of-freedom are denoted as u_s, u_b, u_o and ϕ, respectively.

From Fig. 2, the relative displacement amplitudes of the structure, u_s^t, and the top of isolator, u_b^t, can be expressed as

$$u_s^t = u_o + h\phi + u_s \tag{1a}$$

$$u_b^t = u_o + u_b \tag{1b}$$

where h is the equivalent structural height, defined as the height of the (SDOF) system that approximates the structure. The mass of the structure is assumed to be concentrated at the height h. Usually, h is taken as equal to the structural height for single-story buildings, while for multi-story buildings it can approximately set equal to 0.7 times the total height of the building [48]. The height of the isolator h_b has been considered as negligible compared with h.

Assuming a harmonic ground motion excitation $u_g \cdot e^{i\omega t}$, Lagrange's equations are used to obtain the equation of motion of the system in a matrix form, as elaborated in the Appendix

$$\begin{bmatrix} \left(\frac{\lambda_1}{\omega^2} - 1\right) & -\frac{\lambda_1}{\omega^2} & -1 & -1 \\ -\gamma \cdot \frac{\lambda_1}{\omega^2} & \left[-(1-\gamma) + \frac{\gamma \cdot \lambda_1 + \lambda_2}{\omega^2}\right] & -(1-\gamma) & 0 \\ -\gamma & -(1-\gamma) & \left(-1 + \frac{\lambda_3}{\omega^2}\right) & -\gamma \\ -1 & 0 & -1 & \left(-1 + \frac{\lambda_4}{\omega^2}\right) \end{bmatrix} \times \begin{Bmatrix} u_s \\ u_b \\ u_o \\ h\varphi \end{Bmatrix} = \begin{Bmatrix} 1 \\ (1-\gamma) \\ 1 \\ 1 \end{Bmatrix} \cdot u_g \tag{2}$$

where u_s, u_b, u_o and $h\phi$ stand for the translational displacement of the structure, isolator displacement, foundation displacement, and rotational displacement of the foundation, respectively, and γ is the mass ratio, given by Eq. (3).

$$\gamma = \frac{m_s}{m_s + m_b} \tag{3}$$

where m_s and m_b are the structural and isolation masses, respectively. The λ_1, λ_2, λ_3 and λ_4 parameters are given by the following expressions:

$$\lambda_1 = \omega_s^2 (1 + 2\zeta_s \mathrm{i}) \tag{4}$$

$$\lambda_2 = \omega_b^2 (1 + 2\zeta_b \mathrm{i}) \tag{5}$$

$$\lambda_3 = \omega_h^2 \left(1 + 2\zeta_h \mathrm{i} + 2\zeta_g \mathrm{i}\right) \tag{6}$$

$$\lambda_4 = \omega_r^2 \left(1 + 2\zeta_r \mathrm{i} + 2\zeta_g \mathrm{i}\right) \tag{7}$$

where ω_i and ζ_i, $i = s, b, h, r$ are the frequency and the damping ratios for the ith degree-of-freedom defined in the Appendix and ζ_g is the hysteretic soil damping ratio.

3. Equivalent 2-DOF system

3.1. Formulation of equations of motion and modal properties

Since the mass of the foundation has been neglected, no inertia forces are developed at the base of the structure corresponding to the two foundation degrees-of-freedom, u_o and ϕ. Therefore, an equivalent fixed-base two-degree-of-freedom (2-DOF) system can be developed in order to investigate the significance of soil–structure interaction on the system response. The procedure requires that the response of the equivalent system fixed-base 2-DOF system, when excited by a harmonic base excitation $\tilde{u}_g e^{i\omega t}$ should coincide with the dynamic response of the initial 4-DOF system. For the equivalent fixed-base 2-DOF system shown in

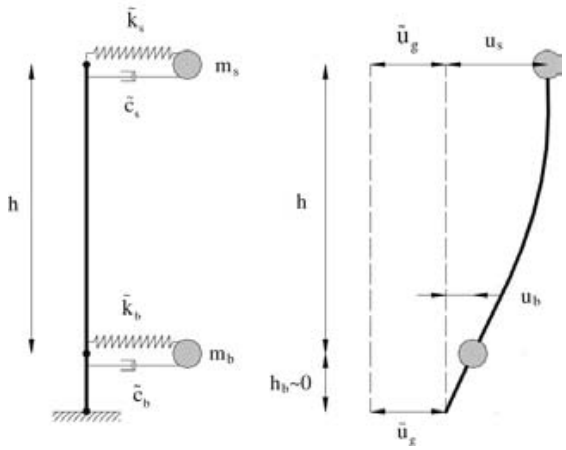

Fig. 3. Equivalent fixed-base 2-DOF system.

Fig. 3, the equations of motion are formulated using the Lagrange's equations, to yield:

$$-m_s \cdot \omega^2 \cdot u_s + \mathrm{i}\omega \cdot \tilde{c}_s (u_s - u_b) + \tilde{k}_s (u_s - u_b) = m_s \cdot \omega^2 \tilde{u}_g \tag{8}$$

$$-m_b \cdot \omega^2 \cdot u_b + \mathrm{i}\omega \cdot \tilde{c}_b u_b - \mathrm{i}\omega \cdot \tilde{c}_s (u_s - u_b) + \tilde{k}_b u_b - \tilde{k}_s (u_s - u_b) = m_b \cdot \omega^2 \tilde{u}_g. \tag{9}$$

The title symbol ($\sim$) denotes the parameters of the equivalent system: u_s and u_b are the structural and isolation degrees-of-freedom considered identical with the deformations of the initial system; $\tilde{k}_i$ and $\tilde{c}_i$ are the stiffness and damping coefficients of the ith degree-of-freedom and $\tilde{u}_g$ is the amplitude of the equivalent input ground motion. Using the following expression for the damping ratios and frequencies for the equivalent system:

$$\tilde{\zeta}_b = \frac{\omega \cdot \tilde{c}_b}{2\tilde{k}_b}, \qquad \tilde{\zeta}_s = \frac{\omega \cdot \tilde{c}_s}{2\tilde{k}_s}, \qquad \tilde{\omega}_b^2 = \frac{\tilde{k}_b}{m_b + m_s}, \qquad \tilde{\omega}_s^2 = \frac{\tilde{k}_s}{m_s}. \tag{10}$$

Eqs. (8) and (9) can be written as

$$\left[1 + 2\tilde{\zeta}_s \mathrm{i} - \frac{\omega^2}{\tilde{\omega}_s^2}\right] u_s - \left(1 + 2\tilde{\zeta}_s \mathrm{i}\right) u_b = \frac{\omega^2}{\tilde{\omega}_s^2} \tilde{u}_g \tag{11}$$

$$-\left[\frac{\tilde{\omega}_s^2}{\tilde{\omega}_b^2} \cdot \gamma \left(1 + 2\tilde{\zeta}_s \mathrm{i}\right)\right] u_s + \left[1 + 2\tilde{\zeta}_b \mathrm{i} + \frac{\tilde{\omega}_s^2}{\tilde{\omega}_b^2} \cdot \gamma \left(1 + 2\tilde{\zeta}_s \mathrm{i}\right) - (1-\gamma) \frac{\omega^2}{\tilde{\omega}_b^2}\right] u_b = (1-\gamma) \frac{\omega^2}{\tilde{\omega}_b^2} \tilde{u}_g. \tag{12}$$

The equations of motion for the equivalent 2-DOF system can be cast in the following matrix form:

$$\left(\left[\tilde{\mathrm{K}}\right] + \mathrm{i} \cdot \left[\tilde{\zeta}\right]\right) \begin{Bmatrix} u_s \\ u_b \end{Bmatrix} = \begin{Bmatrix} \frac{\omega^2}{\tilde{\omega}_s^2} \\ (1-\gamma) \frac{\omega^2}{\tilde{\omega}_b^2} \end{Bmatrix} \tilde{u}_g \tag{13}$$

where the complex stiffness matrix of the equivalent 2-DOF system is given by

$$\left(\left[\tilde{\mathrm{K}}\right] + \mathrm{i} \cdot \left[\tilde{\zeta}\right]\right) = \begin{bmatrix} 1 + 2\tilde{\zeta}_s \mathrm{i} - \frac{\omega^2}{\tilde{\omega}_s^2} & -\left(1 + 2\tilde{\zeta}_s \mathrm{i}\right) \\ -\frac{\tilde{\omega}_s^2}{\tilde{\omega}_b^2} \gamma \left(1 + 2\tilde{\zeta}_s \mathrm{i}\right) & 1 + 2\tilde{\zeta}_b \mathrm{i} + \frac{\tilde{\omega}_s^2}{\tilde{\omega}_b^2} \gamma \left(1 + 2\tilde{\zeta}_s \mathrm{i}\right) - (1-\gamma) \frac{\omega^2}{\tilde{\omega}_b^2} \end{bmatrix}. \tag{14}$$

The eigenfrequencies and natural modes of the equivalent fixed-base 2-DOF system can be determined by setting $\tilde{\zeta}_b = \tilde{\zeta}_s = 0$ and $\omega = \tilde{\omega}_m$ in Eqs. (13) and (14) and by imposing the determinant of the stiffness matrix to be equal to zero, to yield the following characteristic equation for the equivalent system:

$$b_1 \cdot \tilde{\omega}_m^4 + b_2 \cdot \tilde{\omega}_m^2 + b_3 = 0 \tag{15}$$

where

$$b_1 = (1-\gamma), \qquad b_2 = -(\tilde{\omega}_s^2 + \tilde{\omega}_s^2 \cdot \gamma \cdot \tilde{R}_s) \quad \text{and} \quad b_3 = \tilde{\omega}_s^4 \cdot \gamma \cdot \tilde{R}_s \tag{16}$$

$\tilde{\omega}_{1,2}^2, m = 1, 2$ are the natural frequencies of the isolation and structural mode, respectively. The parameter $\tilde{R}_s$ denotes the stiffness ratio of the equivalent system, that is

$$\tilde{R}_s = \frac{\tilde{k}_b}{\tilde{k}_s}. \tag{17}$$

By means of $\tilde{R}_s$ the frequency ratio can be expressed as

$$\frac{\tilde{\omega}_b^2}{\tilde{\omega}_s^2} = \gamma \cdot \tilde{R}_s. \tag{18}$$

Solving Eq. (16) yields the eigenfrequencies

$$\tilde{\omega}_{1,2}^2 = \frac{-b_2 \mp \sqrt{b_2^2 - 4 \cdot b_1 \cdot b_3}}{2 \cdot b_1}. \tag{19}$$

The corresponding eigenmodes are given by

$$\{\tilde{\Phi}^i\} = \begin{Bmatrix} \tilde{\Phi}_s^i \\ \tilde{\Phi}_b^i \end{Bmatrix} = \begin{Bmatrix} 1 \\ 1-\tilde{\alpha}_i \end{Bmatrix}, \quad \text{where: } \tilde{\alpha}_i = \frac{\tilde{\omega}_i^2}{\tilde{\omega}_s^2} \text{ with } i = 1, 2 \tag{20}$$

where $\{\tilde{\Phi}^1\}$ and $\{\tilde{\Phi}^2\}$ are the isolation and structural mode, respectively. The effective modal mass ratios are given by

$$\frac{m_{\text{eff},i}}{m_b + m_s} = \frac{1}{m_b + m_s} \frac{\left(\{\tilde{\Phi}^i\}^{\mathrm{T}} \left[\tilde{M}\right] \begin{Bmatrix} 1 \\ 1 \end{Bmatrix}\right)^2}{\{\tilde{\Phi}^i\}^{\mathrm{T}} \left[\tilde{M}\right] \{\tilde{\Phi}^i\}} = \frac{\left[\gamma + (1-\tilde{\alpha}_i) \cdot (1-\gamma)\right]^2}{\gamma + (1-\tilde{\alpha}_i)^2 \cdot (1-\gamma)}, \quad i = 1, 2. \tag{21}$$

3.2. Damping ratios of equivalent system

In order develop the damping and frequency characteristics of the equivalent system, in terms of the response characteristics of the initial system, the following procedure is applied. Similarly to Eqs. (17) and (18), valid for the equivalent 2-DOF system, the stiffness and frequency ratios for the initial system are given by the expressions

$$R_s = \frac{k_b}{k_s}, \qquad \frac{\omega_b^2}{\omega_s^2} = \gamma \cdot R_s. \tag{22}$$

The translational, u_h, and rotational displacement of the foundation, $h\phi$, can be expressed in terms of u_s and u_b, by performing a series of algebraic calculations using Eq. (2) as follows:

$$u_o = \frac{\omega_b^2}{\omega_h^2} \frac{1 + 2\zeta_b \cdot \mathrm{i}}{1 + 2\zeta_h \cdot \mathrm{i} + 2\zeta_g \cdot \mathrm{i}} u_b = \frac{\lambda_2}{\lambda_3} u_b \tag{23}$$

$$h \cdot \phi = \frac{\omega_s^2}{\omega_r^2} \frac{1 + 2\zeta_s \cdot \mathrm{i}}{1 + 2\zeta_r \cdot \mathrm{i} + 2\zeta_g \cdot \mathrm{i}} u_s - \frac{\omega_s^2}{\omega_r^2} \frac{1 + 2\zeta_s \cdot \mathrm{i}}{1 + 2\zeta_r \cdot \mathrm{i} + 2\zeta_g \cdot \mathrm{i}} u_b = \frac{\lambda_1}{\lambda_4} u_s - \frac{\lambda_1}{\lambda_4} u_b \tag{24}$$

where $\omega_i, \zeta_i, i = s, b, h, r$ are defined in the Appendix. Substituting Eqs. (23) and (24) into the first two equations of the system described by Eq. (2) yields

$$\left[\frac{\lambda_1}{\omega^2} - \frac{\lambda_1}{\lambda_4} - 1\right] u_s + \left[-\frac{\lambda_1}{\omega^2} + \frac{\lambda_1}{\lambda_4} - \frac{\lambda_2}{\lambda_4}\right] u_b = u_g \tag{25}$$

$$-\left[\frac{\lambda_1}{\omega^2} \cdot \gamma\right] u_s + \left[-(1-\gamma) + \frac{\lambda_2}{\omega^2} - (1-\gamma)\frac{\lambda_2}{\lambda_3} + \frac{\lambda_1}{\omega^2} \cdot \gamma\right] u_b = (1-\gamma)\, u_g. \tag{26}$$

Neglecting the second order terms that involve damping ratio products and taking into consideration Eqs. (4)–(7), the following expressions are derived

$$\left[1 + 2\zeta_s \cdot \mathrm{i} - \frac{\omega^2}{\omega_r^2}\left(1 + 2\zeta_s \cdot \mathrm{i} - 2\zeta_r \cdot \mathrm{i} - 2\zeta_g \cdot \mathrm{i}\right) - \frac{\omega^2}{\omega_s^2}\right] u_s + \left[-(1 + 2\zeta_s \cdot \mathrm{i}) + \frac{\omega^2}{\omega_r^2}\left(1 + 2\zeta_s \cdot \mathrm{i} - 2\zeta_r \cdot \mathrm{i} - 2\zeta_g \cdot \mathrm{i}\right) - \frac{\omega_b^2 \omega^2}{\omega_h^2 \cdot \omega_s^2}\left(1 + 2\zeta_b \mathrm{i} - 2\zeta_h \cdot \mathrm{i} - 2\zeta_g \cdot \mathrm{i}\right)\right] u_b = \frac{\omega^2}{\omega_s^2} u_g \tag{27}$$

$$\left[-(1-\gamma)\frac{\omega^2}{\omega_b^2} - (1-\gamma)\frac{\omega^2}{\omega_h^2}\left(1 + 2\zeta_b \mathrm{i} - 2\zeta_h \mathrm{i} - 2\zeta_g \mathrm{i}\right) + (1 + 2\zeta_b \mathrm{i}) + \frac{\omega_s^2}{\omega_b^2} \cdot \gamma\,(1 + 2\zeta_s \mathrm{i})\right] u_b - \left[\frac{\omega_s^2}{\omega_b^2} \cdot \gamma\,(1 + 2\zeta_s \mathrm{i})\right] u_s = (1-\gamma)\frac{\omega^2}{\omega_b^2} u_g. \tag{28}$$

The expressions (27) and (28) include only the two dynamic degrees of freedom, u_s and u_b, and can be considered as equivalent to Eqs. (11) and (12). Equating the second parts of Eqs. (11) and (27) as well as the coefficients of u_s and u_b yields to the following relations:

$$\left[1 + 2\zeta_s \cdot \mathrm{i} - \frac{\omega^2}{\omega_r^2}\left(1 + 2\zeta_s \cdot \mathrm{i} - 2\zeta_r \cdot \mathrm{i} - 2\zeta_g \cdot \mathrm{i}\right) - \frac{\omega^2}{\omega_s^2}\right] = \left[1 + 2\tilde{\zeta}_{11}\mathrm{i} - \frac{\omega^2}{\tilde{\omega}_s^2}\right] \tag{29}$$

$$\left[-(1 + 2\zeta_s \cdot \mathrm{i}) + \frac{\omega^2}{\omega_r^2}\left(1 + 2\zeta_s \cdot \mathrm{i} - 2\zeta_r \cdot \mathrm{i} - 2\zeta_g \cdot \mathrm{i}\right) - \frac{\omega_b^2 \omega^2}{\omega_h^2 \cdot \omega_s^2}\left(1 + 2\zeta_b \mathrm{i} - 2\zeta_h \cdot \mathrm{i} - 2\zeta_g \cdot \mathrm{i}\right)\right] = -\left(1 + 2\tilde{\zeta}_{12}\mathrm{i}\right) \tag{30}$$

$$\frac{\omega^2}{\omega_s^2} u_g = \frac{\omega^2}{\tilde{\omega}_s^2} \tilde{u}_g. \tag{31}$$

Also, equating the real and imaginary parts in Eqs. (29) and (30) results in

$$\frac{1}{\tilde{\omega}_s^2} = \frac{1}{\omega_s^2} + \frac{1}{\omega_r^2} \tag{32a}$$

$$\frac{\omega^2}{\omega_r^2} - \frac{\omega^2 \omega_b^2}{\omega_h^2 \omega_s^2} = 0 \tag{32b}$$

$$\tilde{\zeta}_{s11} = \zeta_s\left(1 - \frac{\omega^2}{\omega_r^2}\right) + \frac{\omega^2}{\omega_r^2} \cdot \zeta_r + \frac{\omega^2}{\omega_r^2} \cdot \zeta_g \tag{32c}$$

$$\tilde{\zeta}_{s12} = \zeta_s\left(1-\frac{\omega^2}{\omega_r^2}\right)+\frac{\omega^2}{\omega_r^2}\cdot\zeta_r + \frac{\omega^2\cdot R_s\cdot\gamma}{\omega_r^2}\cdot\zeta_b+\frac{\omega^2\cdot R_s\cdot\gamma}{\omega_r^2}\cdot\zeta_h. \tag{32d}$$

Following the same procedure for Eqs. (12) and (28) one obtains

$$\frac{\omega_s^2}{\omega_b^2}=\frac{\tilde{\omega}_s^2}{\tilde{\omega}_b^2} \tag{33a}$$

$$\frac{1}{\tilde{\omega}_b^2}=\frac{1}{\omega_b^2}+\frac{1}{\omega_h^2} \tag{33b}$$

$$\tilde{\zeta}_{s21}=\zeta_s \tag{33c}$$

$$\tilde{\zeta}_{b22}+\frac{1}{\tilde{R}_s}\tilde{\zeta}_{s22} = \left[1-(1-\gamma)\frac{\omega^2}{\omega_h^2}\right]\cdot\zeta_b+(1-\gamma)\frac{\omega^2}{\omega_h^2}\cdot\zeta_h + (1-\gamma)\frac{\omega^2}{\omega_h^2}\cdot\zeta_g+\frac{\zeta_s}{\tilde{R}_s}. \tag{33d}$$

In view of Eqs. (22), (32a) and (33b) and the circular frequencies ω_h, ω_r, ω_s and ω_b of the translational, rotational, structural and isolation degree-of-freedom, respectively, expressed by

$$\omega_h^2=\frac{k_h}{m_b+m_s},\quad \omega_r^2=\frac{k_r}{m_s h^2},\quad \omega_s^2=\frac{k_s}{m_s},\quad \omega_b^2=\frac{k_b}{m_b+m_s} \tag{I-7}$$

where k_i is the stiffness coefficient of the ith degree of freedom, the $\tilde{\omega}_s^2$ and $\tilde{\omega}_b^2$ can be calculated from

$$\tilde{\omega}_s^2=\frac{R_s}{\frac{k_b}{k_r}\cdot h^2+R_s}\omega_s^2 \tag{34}$$

$$\tilde{\omega}_b^2=\frac{\gamma\cdot R_s}{\frac{k_s}{k_r}\cdot h^2+1}\omega_s^2 \tag{35}$$

by means of which the $\tilde{\omega}_s^2$ and $\tilde{\omega}_b^2$ can be expressed in terms of the stiffness and mass characteristics of the initial 4-DOF system. Consequently, considering that: (i) the degrees-of-freedom corresponding to the structure and the isolation have the same amplitudes for both systems, and (ii) the response of the initial and the equivalent system are equal at resonance, an equivalent damping ratio $\left[\tilde{\zeta}\right]$ can be obtained in a matrix form from Eqs. (32c), (32d), (33c) and (33d)

$$\left[\tilde{\zeta}\right]=\begin{bmatrix}\tilde{\zeta}_{s11} & -\tilde{\zeta}_{s12}\\ -\frac{\tilde{\zeta}_{s21}}{\tilde{R}_s} & \tilde{\zeta}_{b22}+\frac{1}{\tilde{R}_s}\tilde{\zeta}_{s22}\end{bmatrix}. \tag{36}$$

4. Modal properties and damping ratios with SSI parameters

In this study, the following frequency-independent expressions for the foundation stiffness and damping coefficients are adopted for a rigid circular disk on a homogenous stratum underlain by bedrock at shallow depth [49]:

$$k_h=\frac{8G\alpha}{2-v}\left(1+\frac{1}{2\tilde{H}}\right)\qquad c_h=\frac{4.6\alpha^2}{2-v}\cdot\rho\cdot V_s \tag{37}$$

$$k_r=\frac{8G\alpha^3}{3(1-v)}\left(1+\frac{1}{6\tilde{H}}\right)\qquad c_r=\frac{0.4\alpha^4}{1-v}\cdot\rho\cdot V_s \tag{38}$$

where α is a characteristic dimension of the foundation, G, v, ρ and V_s are the soil material shear modulus, Poisson's ratio, mass density and shear wave velocity, respectively; H is the thickness of the soil stratum and $\tilde{H}$ is the ratio of the soil stratum thickness H to the characteristic dimension α of the foundation. In the limiting case of a very deep soil formation, that is $\tilde{H}\to\infty$, Eqs. (37) and (38) yield the corresponding expressions for a soil halfspace. In order to evaluate the effect of SSI on the overall response, the following dimensionless parameters are introduced:

$$\bar{s}=\frac{\omega_s h}{V_s},\qquad \bar{h}=\frac{h}{\alpha},\qquad \bar{m}=\frac{m_b+m_s}{\rho\alpha^3}. \tag{39}$$

The parameter $\bar{s}$ is a stiffness ratio expressing the relative stiffness between structure and soil, $\bar{m}$ is a mass ratio denoting the relation between a characteristic soil mass and the mass of the overall isolation–structure system. The parameter α could be the radius or diameter for a cyclical foundation or the lateral dimension of a mat foundation [31]. The assumption of a mat foundation is valid for foundations with aspect ratio less than 4:1 in plan, according to Roesset [50]. Using the $\bar{s}$, $\bar{h}$ and $\bar{m}$ parameters, Eqs. (34) and (35) become:

$$\frac{\tilde{\omega}_s^2}{\omega_s^2}=\eta \tag{40}$$

$$\frac{\tilde{\omega}_b^2}{\omega_s^2}=R_s\cdot\gamma\cdot\eta \tag{41}$$

where

$$\eta=\frac{8\left(1+\frac{1}{6\tilde{H}}\right)}{8\left(1+\frac{1}{6\tilde{H}}\right)+\bar{s}^2\cdot\gamma\cdot\bar{m}\cdot 3(1-v)}. \tag{42}$$

The assumption of equal response for the initial and the equivalent undamped systems leads to equality of the stiffness ratios R_s and $\tilde{R}_s$ [32]. Neglecting the non-diagonal terms according to a procedure proposed by Veletsos and Ventura [51], the generalized damping ratios matrix can be cast in the following form:

$$\left[\tilde{\zeta}^*\right]=\left[\tilde{\Phi}\right]^{\mathrm{T}}\left[\tilde{\zeta}\right]\left[\tilde{\Phi}\right]=\begin{bmatrix}\tilde{\zeta}_1 & 0\\ 0 & \tilde{\zeta}_2\end{bmatrix}, \tag{43}$$

where

$$\tilde{\zeta}_1 = \tilde{\zeta}_{b11}-(1-\tilde{\alpha}_1)\left(\tilde{\zeta}_{b12}+\frac{\tilde{\zeta}_{s21}}{\tilde{R}_s}\right)+(1-\tilde{\alpha}_1)^2\left(\tilde{\zeta}_{b22}+\frac{1}{\tilde{R}_s}\tilde{\zeta}_{s22}\right) \tag{44}$$

$$\tilde{\zeta}_2 = \tilde{\zeta}_{b11}-(1-\tilde{\alpha}_2)\left(\tilde{\zeta}_{b12}+\frac{\tilde{\zeta}_{s21}}{\tilde{R}_s}\right)+(1-\tilde{\alpha}_2)^2\left(\tilde{\zeta}_{b22}+\frac{1}{\tilde{R}_s}\tilde{\zeta}_{s22}\right). \tag{45}$$

5. Numerical examples and parametric study

The variation of the effective modal mass ratios for the first two modes expressed by Eq. (21) is given in Fig. 4. The percentage of the effective mass ratio for the fundamental mode exceeds 90% for the range of $\tilde{R}_s$ between 0 and 1. In the limit, as $\tilde{R}_s\to 0$ the isolation stiffness can be considered as negligible compared with the building stiffness, a case that corresponds to a relatively stiff structure. The limit case: $\tilde{R}_s\to 1$ corresponds to a building and isolation system with similar stiffness, e.g., slender and tall buildings. Three representative values for γ have been considered: (i) $\gamma=0.5$: it corresponds to a single story base-isolated building,

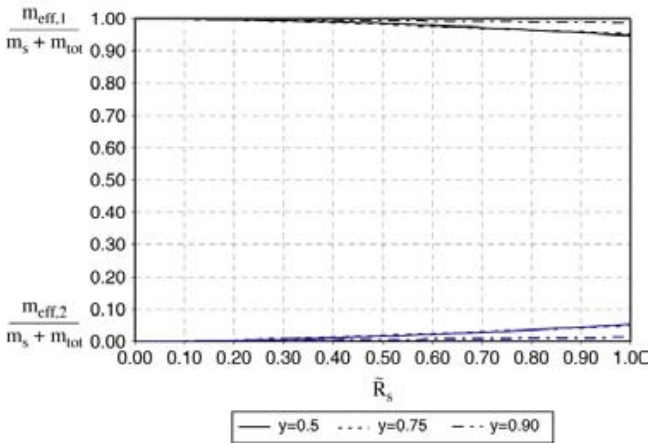

Fig. 4. Effective modal mass ratios for the isolation and structural mode.

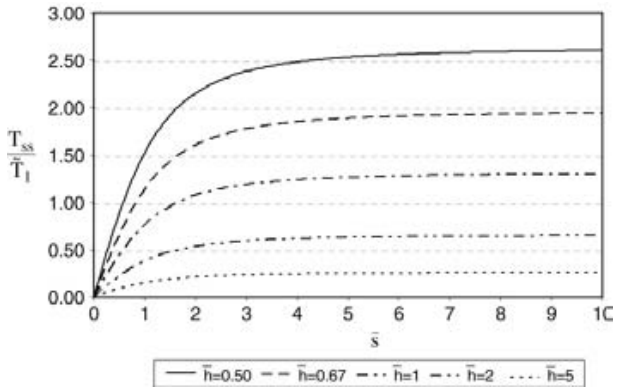

Fig. 5. Variation of $Tss/\tilde{T}_1$ for representative $\bar{h}$ ($\gamma = 0.75$, $R_s = 0.2$, $v = 0.33$, $\bar{m} = 3$, $\zeta_b = 25\%$, $\zeta_s = 2\%$, $\zeta_g = 5\%$, $\bar{H} = 4$).

where the isolation mass, m_b, is half of the total mass, $m_s + m_b$, (ii) $\gamma = 0.9$: it expresses a multistory building where m_b is relatively small compared with the structural mass m_s, and (iii) $\gamma = 0.75$ depicting an intermediate relation between m_s and m_b. From Fig. 4 one can conclude that the response of the equivalent system is almost entirely determined from the first mode, the so-called isolation mode. Thus, it can be deduced that the modal damping ratio, $\tilde{\zeta}_1$, can adequately describe the overall foundation–isolation–structure system behavior.

An investigation of the effect of the various parameters on the equivalent system stiffness and damping characteristics is discussed in what follows. The structural damping ratio ζ_s is set equal to 2%, since the structure is anticipated to remain plastically elastic during ground shaking. The isolation damping ratio ζ_b is set equal either to 25% or 5% and the soil damping ratio ζ_g is set equal to 5%, corresponding to a small-to-moderate soil strain level.

Figs. 5–7 present the variation of the ratio $T_{ss}/\tilde{T}_1$, where T_{ss} is the soil stratum fundamental period and $\tilde{T}_1$ is the equivalent two-degree-of-freedom system fundamental period corresponding to $\tilde{\omega}_1$ given by Eq. (19). The soil fundamental period is given by [52]

$$T_{ss} = \frac{4H}{V_s}. \tag{46}$$

Generally, the effects of SSI on the structural behavior are considered insignificant when the equivalent system fundamental period becomes smaller than T_{ss}. It can be observed from Figs. 5–7 that the larger $\bar{s}$ is, the larger the $T_{ss}/\tilde{T}_1$ ratio, since for a given R_s ratio both the structure and isolation become stiffer in comparison with the soil layer. As shown in Fig. 5 for the case of $\bar{m} = 3$, the

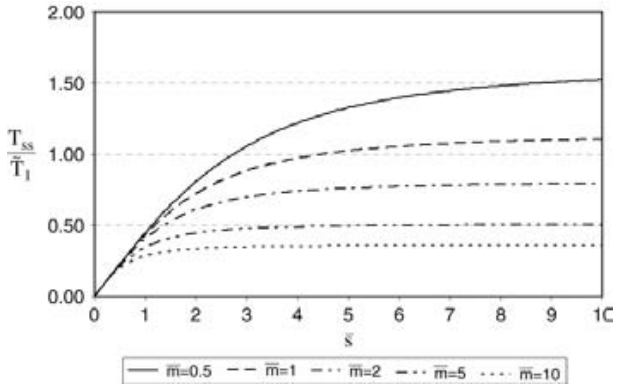

Fig. 6. Variation of $Tss/\tilde{T}_1$ for representative $\bar{m}$ ($\gamma = 0.75$, $R_s = 0.2$, $v = 0.33$, $\bar{h} = 2$, $\zeta_b = 25\%$, $\zeta_s = 2\%$, $\zeta_g = 5\%$, $\bar{H} = 4$).

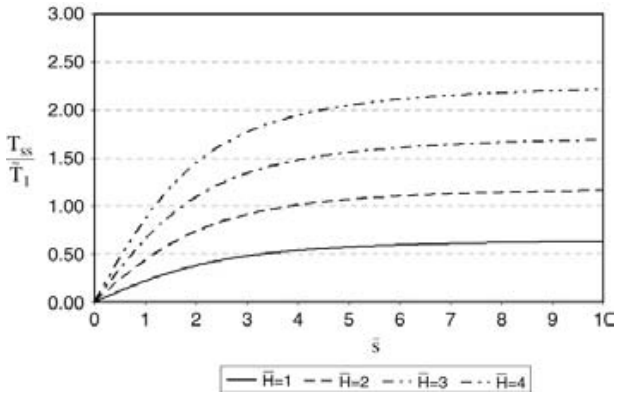

Fig. 7. Variation of $Tss/\tilde{T}_1$ for representative $\bar{H}$ ($\gamma = 0.75$, $R_s = 0.2$, $v = 0.33$, $\bar{h} = 1$, $\zeta_b = 25\%$, $\zeta_s = 2\%$, $\zeta_g = 5\%$, $\bar{m} = 1$).

ratio $T_{ss}/\tilde{T}_1$ becomes greater than one for relatively stiff buildings with low $\bar{h}$ ($\bar{h} < 1.0$), that is, when the effective height of the structure is small compared with a characteristic dimension of the foundation. The $T_{ss}/\tilde{T}_1$ ratio changes significantly with $\bar{s}$, specially for $\bar{s}$ varying between 0.5 and 3.5. For $\bar{s} > 4$ the relative stiffness of soil and structure expressed by a further increase in $\bar{s}$ appears to be insignificant in affecting the fundamental period of the equivalent structure-isolation system. For structures with slenderness ratio $\bar{h} > 1$, $T_{ss}/\tilde{T}_1$ does not exceed unity, which implies that SSI effects become negligible.

Fig. 6 shows the variation of $T_{ss}/\tilde{T}_1$ with $\bar{s}$ for several values of the mass ratio $\bar{m}$ and representative values of γ, R_s, $\bar{h}$ and $\bar{H}$. An $\bar{h} = 2$ slenderness ratio has been considered and a relatively deep soil stratum $\bar{H} = 4$ compared with the foundation characteristic dimension have been used. The structure stiffness has been considered significantly greater than the isolation stiffness expressed by $R_s = 0.2$. For structures with relatively large mass $\bar{m} > 2$, the $T_{ss}/\tilde{T}_1$ ratio never exceeds unity, which implies that SSI effects are more pronounced for light structures. In the range of $\bar{s} < 2$ no consideration of SSI is required independently of the mass ratio of the structure. In Fig. 7 the $T_{ss}/\tilde{T}_1$ ratio is plotted for representative $\bar{H}$ values in the range between one and four. An increase in the soil thickness leads to a more flexible soil stratum and thus to smaller values of $T_{ss}/\tilde{T}_1$. For $\bar{s} < 1$ the effects of SSI are negligible, regardless of the thickness of the soil stratum. From Figs. 5–7 one may conclude that SSI becomes significant for relatively squat structures with a small mass founded on loose soils, especially for soil layers with a relatively large thickness ($\bar{H} > 2$). The variation of the ratio $\tilde{\omega}_1/\omega_s$ is shown in Fig. 8 for a relatively squat structure with a slenderness ratio $\bar{h} = 1$ resting on

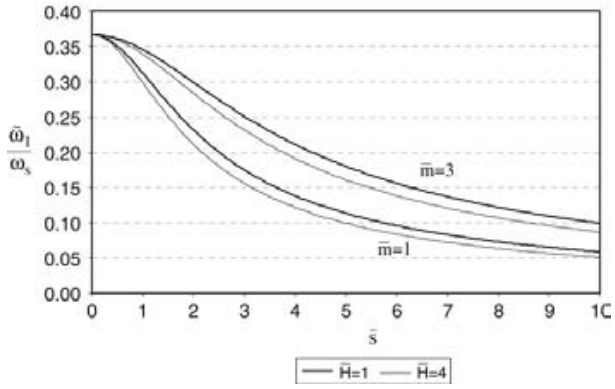

Fig. 8. Variation of $\tilde{\omega}_1/\omega_s$ for representative $\bar{H}$ and $\bar{m}$ ($\gamma = 0.75$, $R_s = 0.2$, $v = 0.33$, $\bar{h} = 1$, $\zeta_b = 25\%$, $\zeta_s = 2\%$, $\zeta_g = 5\%$).

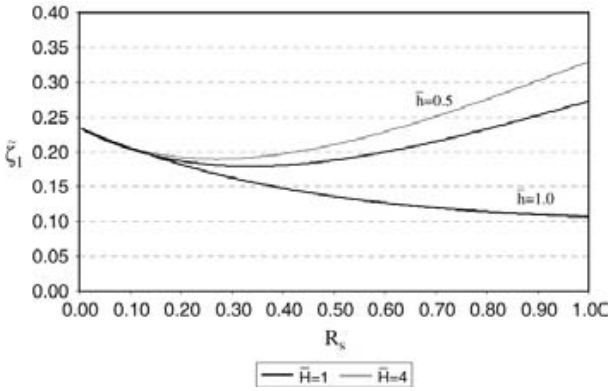

Fig. 9. Variation of composite damping ratio $\tilde{\zeta}_1$ with R_s for representative $\bar{h}$, $\bar{H}$ ($\bar{s} = 5$, $\gamma = 0.75$, $v = 0.33$, $\zeta_b = 5\%$, $\zeta_s = 2\%$, $\zeta_g = 5\%$, $\bar{m} = 3$).

a soil layer with $\bar{H} = 1$ and 4. The $\tilde{\omega}_1/\omega_s$ ratio appears to decrease with the $\bar{s}$. The variation of $\tilde{\omega}_1/\omega_s$ is not affected by the change in the layer thickness for the moderate values of $\bar{H}$ plotted in Fig. 8. For $\bar{m} = 3$ corresponding to relatively large structural mass, the $\tilde{\omega}_1/\omega_s$ ratio seems to decrease in a smoother rate with $\bar{s}$ compared with smaller values of $\bar{m}$.

Fig. 9 shows the variation of the composite damping ratio $\tilde{\zeta}_1$ with the stiffness ratio R_s. For relatively slender structures, $\tilde{\zeta}_1$ decreases as the isolator stiffness increases for a constant structural stiffness, and the layer thickness is not critical in affecting $\tilde{\zeta}_1$. Independently of $\bar{h}$, and for $R_s < 0.25$, the damping ratio is insignificantly affected by either the slenderness ratio or the thickness of the soil stratum. In Figs. 10 and 11 the damping ratio $\tilde{\zeta}_1$ is plotted as a function of $\bar{s}$. It is observed that the effect of the soil stratum thickness is pronounced for small $\bar{h}$ that corresponds to stiff structures. It is also observed that the slenderness ratio is more significant in affecting the damping ratio. When the fundamental frequency of the site $\tilde{\omega}_1$ is smaller than the cut-off frequency $\pi V_s/2H$, no radiation damping should be considered in estimating the composite damping ratio, i.e., $\zeta_r = \zeta_h = 0$ [22]. Concerning this special case Figs. 10–12 include the "*no-radiation*" curves. From Fig. 10 it can be deduced that parameter $\bar{H}$ is not influential, even for the case of very squat structures with low slenderness ratio ($\bar{h} = 0.5$) and low structural mass ($\bar{m} = 1$). For relatively small values of the stiffness ratio $\bar{s} < 1$, no significant change is observed of the composite damping ratio $\tilde{\zeta}_1$. In Fig. 10 it is observed that $\tilde{\zeta}_1$ is lower than the selected isolation damping ζ_b taken as 25%, especially for lower values of $\bar{s}$. For large values of $\bar{s} > 3$, the effects of SSI on the composite damping ratio greatly depends on the slenderness ratio. When no radiation damping is considered, no significant change of the composite damping ratio with $\bar{s}$ is observed for relatively slender structures ($\bar{h} = 1.0$). Also, note that for lower values of slenderness ratio $\tilde{\zeta}_1$ decreases with $\bar{s}$. The observations concerning the variation of $\tilde{\zeta}_1$ with $\bar{s}$ are also valid for the cases depicted in Fig. 11. Comparison of Fig. 10 with Fig. 11 shows that an increase of the mass ratio $\bar{m} = 3$ slightly decreases the equivalent damping ratio of the system $\tilde{\zeta}_1$.

It should be mentioned that the composite damping ratio is significantly affected by the isolation system damping ratio. This fact is demonstrated by comparing Fig. 12, which presents the variation of the composite damping ratio for an isolation damping ratio, $\zeta_b = 5\%$ and a damping ratio $\tilde{\zeta}_1$ varying between 3% and 12%, Fig. 10 where $\tilde{\zeta}_1$ varies between 17% and 23% for the same slenderness ratio variation $0.5 \leq \bar{h} \leq 1.0$. As anticipated, the influence of the slenderness ratio $\bar{h}$ on $\tilde{\zeta}_1$ diminishes for vanishing radiation, for fundamental frequencies below the cut-off frequency of the site. When radiation damping is insignificant, and for low

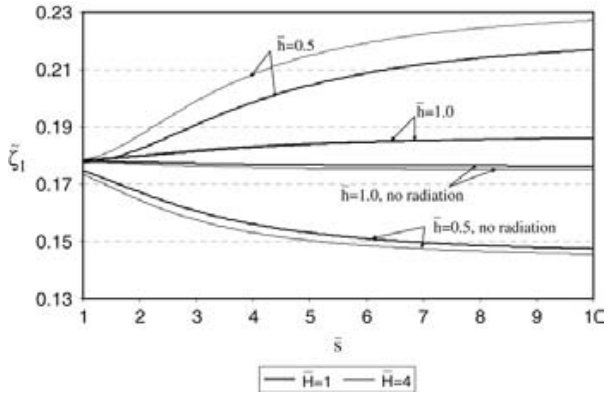

Fig. 10. Variation of composite damping ratio $\tilde{\zeta}_1$ with $\bar{s}$ for representative $\bar{h}$, $\bar{H}$ and $\bar{m} = 1$($\bar{R}_s = 0.2$, $\gamma = 0.75$, $v = 0.33$, $\zeta_b = 25\%$, $\zeta_s = 2\%$, $\zeta_g = 5\%$).

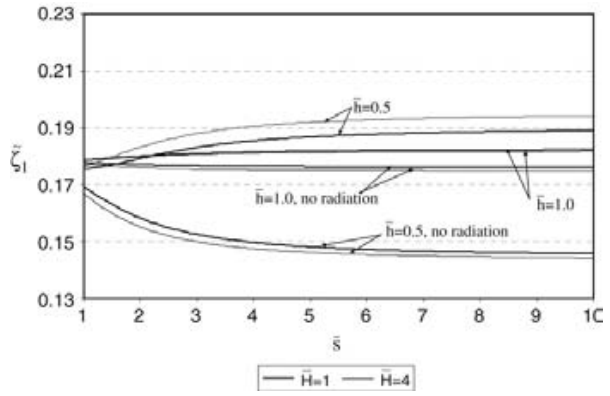

Fig. 11. Variation of composite damping ratio $\tilde{\zeta}_1$ with $\bar{s}$ for representative $\bar{h}$, $\bar{H}$ and $\bar{m} = 3$ ($\bar{R}_s = 0.2$, $\gamma = 0.75$, $v = 0.33$, $\zeta_b = 25\%$, $\zeta_s = 2\%$, $\zeta_g = 5\%$).

values of isolation damping, the variation of slenderness ratio slightly affects the variation of $\tilde{\zeta}_1$.

It is evident that a more accurate analysis should include the frequency dependence of the impedance functions. In that case, the significance of the soil stratum thickness in affecting the response of the overall system is expected to be more pronounced when a shallow stratum is considered, since significant fluctuations that are relative to the natural frequencies of the stratum are observed in the dynamic stiffness and damping coefficients [53]. Furthermore, when high frequency structures are considered, a significant error can be introduced by neglecting the frequency dependence of the real part of the impedance function [54]. However, for relatively small frequency excitations (i.e. when the

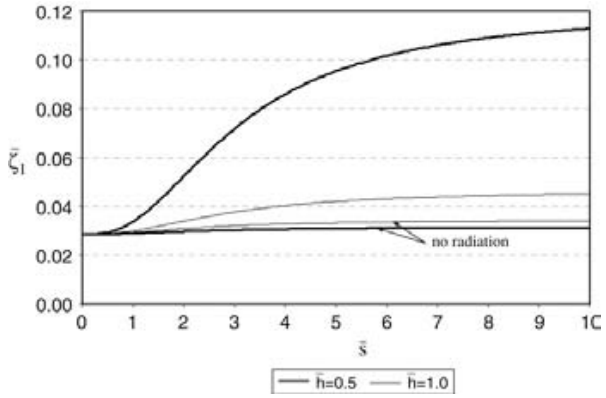

Fig. 12. Variation of composite damping ratio $\tilde{\zeta}_1$ for representative $\bar{h}$ ($\gamma = 0.75$, $R_s = 0.2$, $v = 0.33$, $\zeta_b = 5\%$, $\zeta_s = 2\%$, $\zeta_g = 5\%$, $\bar{m} = 1$, $\bar{H} = 4$).

characteristic dimension of the footing is small compared with the wavelength of the excitation) and, for a relatively deep soil stratum, the conclusions of the study can be considered as valid. For a quantitative evaluation of the issue, a detailed analysis should be performed, a task that could be the subject of a future study.

6. Conclusions

A series of analytical expressions is derived in order to investigate the conditions under which SSI could play a significant role on the response of base-isolated buildings. A simple analytical model — yet one which is capable of describing the most salient system characteristics — is developed. More specifically, assuming a massless foundation system, the equations of motion are derived in the frequency domain for a 4-DOF structure-base isolation-foundation system.

Considering an equivalent fixed-based 2-DOF system, on which an identical structural and base isolation response to the initial 4-DOF is imposed, a series of parametric studies is performed. It can be concluded that: (i) the effects of SSI appear to be significant for squat structures with small mass ratios, that is, buildings with a few stories founded on soft soil layers. (ii) The response greatly depends on the fundamental "isolation" mode, as discussed in Section 5. (iii) SSI affects the modal properties of the system, but has little effect on damping, especially for slender structures. The small effect on damping could be attributed to the significant reduction in the structural stiffness caused by the addition of the flexible isolation system. Thus, the composite damping ratio of the system $\tilde{\zeta}_1$ is strongly influenced by the isolation system damping ratio ζ_b. (iv) The slenderness of the structure appears to be more significant in affecting the damping ratio compared with the soil stratum thickness. (v) When radiation damping is practically zero, the significance of slenderness ratio in affecting the composite damping ratio diminishes for small values of isolation damping.

The methodology presented in this study can be used to estimate the anticipated response of a system, at least at a preliminary design level, for the selection of the appropriate isolation system parameters.

Acknowledgments

The research of Ch.A. Maniatakis is funded by a doctoral scholarship from the Alexander S. Onassis Public Benefit Foundation. This financial support is gratefully acknowledged.

Appendix. Formulation of the equations of motion for the 4-DOF system

Lagrange's equations are used to formulate the equations of motion of the system

$$\frac{\mathrm{d}}{\mathrm{d}t}\left(\frac{\partial K}{\partial \dot{q}_i}\right) - \frac{\partial K}{\partial q_i} + \frac{\partial U}{\partial q_i} + \frac{\partial D}{\partial \dot{q}_i} = 0 \tag{A.1}$$

where K, U and D are the kinetic, potential and dissipation energy, respectively. In Eq. (A.1), the generalized coordinates u_s, u_b, u_o and ϕ of the system are denoted with q_i,. The i index takes the following values: s, b, o and ϕ corresponding to the structural, isolation, horizontal and rotational degrees-of-freedom. Differentiation with respect to time is depicted with dots. Applying Lagrange's equations, the equations of motion for the 4-DOF are derived in a matrix form

$$\begin{bmatrix} m_s & 0 & m_s & m_s\cdot h \\ 0 & m_b & m_b & 0 \\ m_s & m_b & m_s+m_b & m_s\cdot h \\ m_s\cdot h & 0 & m_s\cdot h & m_s\cdot h^2 \end{bmatrix} \begin{Bmatrix} \ddot{u}_s \\ \ddot{u}_b \\ \ddot{u}_o \\ \ddot{\phi} \end{Bmatrix} + \begin{bmatrix} c_s & -c_s & 0 & 0 \\ -c_s & c_b+c_s & 0 & 0 \\ 0 & 0 & c_h & 0 \\ 0 & 0 & 0 & c_\phi \end{bmatrix} \begin{Bmatrix} \dot{u}_s \\ \dot{u}_b \\ \dot{u}_o \\ \dot{\phi} \end{Bmatrix} + \begin{bmatrix} k_s & -k_s & 0 & 0 \\ -k_s & k_b+k_s & 0 & 0 \\ 0 & 0 & k_h & 0 \\ 0 & 0 & 0 & k_\phi \end{bmatrix} \begin{Bmatrix} u_s \\ u_b \\ u_o \\ \phi \end{Bmatrix} = - \begin{Bmatrix} m_s \\ m_b \\ m_s+m_b \\ m_s\cdot h \end{Bmatrix} \ddot{u}_g \tag{A.2}$$

where k_i and c_i are the stiffness and damping coefficients of the ith degree of freedom and $\ddot{u}_g$ is the acceleration of the ground motion. The structural and isolation masses are denoted as m_s and m_b, respectively.

A harmonic ground motion $u_g \cdot \mathrm{e}^{\mathrm{i}\omega t}$ is assumed for the formulation of the equations of motion in the frequency domain. The base reactions of the foundation system, that is, the horizontal force P_h and the moment M_r developed at the base of the isolator, can be expressed as

$$P_h = k_h\left(1 + 2\cdot\zeta_h\mathrm{i} + 2\cdot\zeta_g\mathrm{i}\right)u_o \tag{A.3}$$

$$M_r = k_r\left(1 + 2\cdot\zeta_r\mathrm{i} + 2\cdot\zeta_g\mathrm{i}\right)\phi \tag{A.4}$$

where ζ_h and ζ_r are the viscous damping ratios in the horizontal and rocking direction of motion, respectively, expressed by Eq. (A.5), and ζ_g is the hysteretic damping ratio for the soil [32].

$$\zeta_h = \frac{\omega\cdot c_h}{2k_h} \qquad \zeta_r = \frac{\omega\cdot c_r}{2k_r}. \tag{A.5}$$

Similarly, the corresponding hysteretic damping ratios ζ_s and ζ_b for the structure and the isolator, respectively, are

$$\zeta_s = \frac{\omega\cdot c_s}{2k_s} \qquad \zeta_b = \frac{\omega\cdot c_b}{2k_b}. \tag{A.6}$$

The circular frequencies ω_h, ω_r, ω_s and ω_b of the translational, rotational, structural and isolation degree-of-freedom, respectively, are expressed by

$$\omega_h^2 = \frac{k_h}{m_b+m_s}, \qquad \omega_r^2 = \frac{k_r}{m_s h^2}, \qquad \omega_s^2 = \frac{k_s}{m_s}, \qquad \omega_b^2 = \frac{k_b}{m_b+m_s}. \tag{A.7}$$

Substituting Eqs. (A.5)–(A.7) into Eq. (A.2) the following four equations are derived, considering a harmonic ground motion, as mentioned above:

$$\left[\gamma\cdot\frac{\omega_s^2}{\omega^2}(1+2\zeta_s\mathrm{i})-\gamma\right]u_s-\left[\gamma\cdot\frac{\omega_s^2}{\omega^2}(1+2\zeta_s\mathrm{i})\right]u_b-\gamma\cdot u_o-\gamma\cdot h\phi=\gamma\cdot u_g \tag{A.8a}$$

$$-\left[\gamma\cdot\frac{\omega_s^2}{\omega^2}(1+2\zeta_s\mathrm{i})\right]u_s+\left[-(1-\gamma)+\frac{\omega_b^2}{\omega^2}(1+2\zeta_b\mathrm{i})+\gamma\frac{\omega_s^2}{\omega^2}(1+2\zeta_s\mathrm{i})\right]u_b-(1-\gamma)\cdot u_o=(1-\gamma)\cdot u_g \tag{A.8b}$$

$$-\gamma u_s-(1-\gamma)\cdot u_b+\left[-1+\frac{\omega_h^2}{\omega^2}\left(1+2\zeta_h\mathrm{i}+2\zeta_g\mathrm{i}\right)\right]\cdot u_o-\gamma\cdot h\varphi=u_g \tag{A.8c}$$

$$-u_s-u_b+\left[-1+\frac{\omega_r^2}{\omega^2}\left(1+2\zeta_r\mathrm{i}+2\zeta_g\mathrm{i}\right)\right]h\phi=u_g\,. \tag{A.8d}$$

The above equations of motion can be rewritten in a more convenient matrix form.

References

[1] Staudacher E, Habacher C, Siegenthaler R. Erdbebensicherung in Baum. Neue Zürcher Zeitung. Technikbeilage. Zürich. Switzerland; 1970.
[2] International Council of Building Officials (ICBO). Uniform Building Code. Whittier (CA); 1991.
[3] Naaseh S. Seismic retrofit of San Francisco city hall: The role of masonry and concrete. In: Proceedings of the 3rd national concrete and masonry engineering conference. vol. 2. 1995. p. 769–95.
[4] Constantinou MC, Kartoum A, Reinhorn AM, Bradford P. Sliding isolation system for bridges: Experimental study. Earthq Spectra 1992;8:321–44.
[5] Kelly JM. Earthquake-resistant design with rubber. New York: Springer-Verlag; 1993.
[6] Skinner RI, Robinson WH, McVerry GH. An introduction to seismic isolation. New York: John Wiley & Sons; 1993.
[7] Tsopelas P, Constantinou MC, Kim YS, Okamota S. Experimental study of FPS system in bridge seismic isolation. Earthq Eng Struct Dyn 1996;25:65–78.
[8] Jangid RS, Kelly JM. Base isolation for near-fault motions. Earthq Eng Struct Dyn 2001;30:691–707.
[9] Hall JF. Discussion on the role of damping in seismic isolation. Earthq Eng Struct Dyn 1999;28:1717–20.
[10] Hall JF, Ryan KL. Isolated buildings and the 1997 UBC near-source factors. Earthq Spectra 2000;16:1717–20.
[11] Zhang Y, Iwan WD. Protecting base-isolated structures from near-field ground motion by tuned interaction damper. J Eng Mech ASCE 2002;128(3):287–95.
[12] Sahasrabudhe S, Nagarajaiah S. Experimental study of sliding base-isolated buildings with magnetorheological dampers in near-fault earthquakes. J Struct Eng ASCE 2005;131(7):1025–34.
[13] Ryan KL, Chopra AK. Approximate analysis methods for asymmetric plan base-isolated buildings. Earthq Eng Struct Dyn 2002;31:33–54.
[14] Ryan KL, Chopra AK. Estimating seismic demands for isolation bearings with building overturning effects. J Struct Eng ASCE 2006;132(7):1118–28.
[15] Naeim F, Kelly JM. Design of seismic isolated structures. New York: John Wiley & Sons INC.; 1999.
[16] International Code Council (ICC). International Building Code. Falls Church (VA); 2000.
[17] European committee for standardization (CEN). Eurocode 8, Design of structures for earthquake resistance. EN 1998. Brussels; 2004.
[18] Johnson JJ. In: Chen WF, Scawthorn C, editors. Soil–structure interaction. Earthquake engineering handbook, Boca Raton: CRC Press; 2003. p. 10.1-10.31 [Chapter 10].
[19] Wong HL, Luco JE. Dynamic response of rigid foundations of arbitrary shape. Earthq Eng Struct Dyn 1976;4:587–97.
[20] Idriss IM, Kennedy RP, Agrawal PK, Hadjian AH, Kausel E, Lysmer J, et al. Analyses for soil–structure interaction effects for nuclear power plants. New York: ASCE; 1979.
[21] Johnson JJ. Soil Structure Interaction (SSI): The status of current analysis methods and research. Lawrence Livermore National Laboratory (LLNL). UCRL-53011. NUREGICR-1780. Washington (DC): US Nuclear Regulatory Commission; 1981.
[22] Wolf JP. Dynamic soil–structure interaction. Englewood Cliffs (NJ): Prentice-Hall; 1985.
[23] Wolf JP. Foundation vibration analysis using simple physical models. Englewood Cliffs (NJ): Prentice-Hall; 1994.
[24] Spyrakos CC, Beskos DE. Dynamic response of flexible strip-foundations by boundary and finite elements. Soil Dyn Earthq Eng 1986;5(2):84–96.
[25] Luco JE. Soil–structure interaction effects on the seismic response of tall chimneys. Soil Dyn Earthq Eng 1986;5:170–7.
[26] Goyal A, Chopra AK. Earthquake analysis of intake-outlet towers including tower–water–foundation–soil interaction. Earthq Eng Struct Dyn 1989;18:325–44.
[27] Spyrakos CC. Seismic behaviour of bridge piers including soil structure interaction. Comput. Structures 1992;43:373–84.
[28] Xu C, Spyrakos CC. Seismic analysis of towers including foundation uplift. Eng Struct 1996;18(4):271–8.
[29] Maekawa K, Pimanmas A, Okamoura H. Nonlinear soil–structure interaction. London: Spon Press; 2003.
[30] Building Seismic Safety Council (BSSC). NEHRP recommended provisions for seismic regulations for new buildings and other structures. FEMA 450. Washington (DC): Federal Emergency Management Agency; 2003.
[31] Spyrakos CC. In: Hall WS, Oliveto G, editors. Soil–structure interaction in practice. Boundary element methods for soil–structure interaction, Dordrecht: Kluwer Academic Publishers; 2003. p. 235–72 [Chapter 5].
[32] Spyrakos CC, Vlassis AG. Effect of soil–structure interaction on seismically isolated bridges. J Earthq Eng 2002;6(3):391–429.
[33] Chaudhary MTA, Abé M, Fujino Y. Identification of soil–structure interaction effect in isolated bridges from earthquake records. Soil Dyn Earthq Eng 2001;21:713–25.
[34] Iemura H, Pradono MH. Passive and semi-active seismic response control of a cable-stayed bridge. J Struct Control 2002;9:189–204.
[35] Tongaonkar NP, Jangid RS. Seismic response of isolated bridges with soil–structure interaction. Soil Dyn Earthq Eng 2003;23:287–302.
[36] Dicleli M, Albhaisi S, Mansour MY. Static soil–structure interaction effects in seismic-isolated bridges. Pract Period Struct Des Constr ASCE 2005;10(1):22–33.
[37] Sarrazin M, Moroni O, Roesset JM. Evaluation of dynamic response characteristics of seismically isolated bridges in Chile. Earthq Eng Struct Dyn 2005;34:425–48.
[38] Seeber R, Fisher FD, Rammerstorfer FG. Analysis of a three-dimensional tank–liquid–soil interaction problem. J Press Vessel Technol ASME 1990;112:28–33.
[39] Haroun MA, Abou-Izzeddine W. Parametric study of seismic soil–tank interaction. 1. Horizontal excitation. J Struct Eng ASCE 1992;118(3):783–97.
[40] Shenton III HW, Hampton FP. Seismic response of isolated elevated water tanks. J Struct Eng ASCE 1999;125(9):965–76.
[41] Kim MK, Lim YM, Cho SY, Cho KH, Lee KW. Seismic analysis of base-isolated liquid storage tanks using the BE–FE–BE coupling technique. Soil Dyn Earthq Eng 2002;22:1151–8.
[42] Cho KH, Kim MK, Lim YM, Cho SY. Seismic response of base-isolated liquid storage tanks considering fluid–structure–soil interaction in time domain. Soil Dyn Earthq Eng 2004;24:839–52.
[43] Kelly JM. Shake table tests of long period isolation system for nuclear facilities at soft soil sites. Report No. UCB/EERC-91/03. University of California at Berkeley; 1991.
[44] Constantinou MC, Kneifati MC. Effect of soil–structure interaction on damping and frequencies of base-isolated structures. In: Proceedings of the 3rd US national conference on earthquake engineering. vol. 1. 1986. p. 671–81.
[45] Novak M, Henderson P. Base-isolated buildings with soil–structure interaction. Earthq Eng Struct Dyn 1989;18:751–65.
[46] Tsai CS, Chen C-S, Chen B-J. Effects of unbounded media on seismic responses of FPS-isolated structures. J Struct Control Health Monit 2004;11:1–20.
[47] Chopra AK. Dynamics of structures: Theory and applications to earthquake engineering. 2nd ed. Upper Saddle River (NJ): Prentice-Hall; 2001.
[48] Priestley MJN. Myths and fallacies in earthquake engineering, revisited. Pavia: Rose School; 2003.
[49] Antes H, Spyrakos CC. In: Beskos DE, Anagnostopoulos SA, editors. Soil–structure interaction. Computer analysis and design of earthquake resistant structures: A handbook, Southampton: Computational Mechanics Publications; 1997. p. 271–332 [Chapter 6].
[50] Roesset JM. A review of soil–structure interaction. In: Johnson JJ, editor. Soil–structure interaction: The status of current analysis methods and research. Rpt. No. NUREG/CR-1780 and UCRL-53011, U.S. Nuclear Regulatory Com., Washington DC, and Lawrence Livermore Lab., Livermore, CA; 1980.
[51] Veletsos AS, Ventura CE. Modal analysis of non-classically damped systems. Earthq Eng Struct Dyn 1986;14:217–43.
[52] Kramer SL. Geotechnical earthquake engineering. Upper Saddle River (NJ): Prentice-Hall; 1996.
[53] Mylonakis G, Nikolaou S, Gazetas G. Footings under seismic loading: Analysis and design issues with emphasis on bridge foundations. Soil Dyn. Earthq. Eng. 2006;26(10):824–54.
[54] Stewart JP, Seed RB, Fenves GL. Seismic soil–structure interaction in buildings. I: Analytical aspects. J Geotech Geoenviron Eng 1999;125:26–37.